Excitation-induced energy shifts in the optical gain spectra of InN quantum dots

M. Lorke' , J. Seebeck, P. Gartner, F. Jahnke' , and S. Schulz

Citation: Appl. Phys. Lett. **95**, 081108 (2009); doi: 10.1063/1.3213543
View online: http://dx.doi.org/10.1063/1.3213543
View Table of Contents: http://aip.scitation.org/toc/apl/95/8
Published by the American Institute of Physics

Excitation-induced energy shifts in the optical gain spectra of InN quantum dots

M. Lorke,[1,a)] J. Seebeck,[1] P. Gartner,[1] F. Jahnke,[1,b)] and S. Schulz[2]
[1]*Institute for Theoretical Physics, University of Bremen, Bremen 28359, Germany*
[2]*Tyndall National Institute, Lee Maltings, Cork, Ireland*

(Received 16 June 2009; accepted 10 August 2009; published online 27 August 2009)

A microscopic theory for the optical absorption and gain spectra of InN quantum-dot systems is used to study the combined influence of material properties and interaction-induced effects. Atomistic tight-binding calculations for the single-particle properties of the self-assembled quantum-dot and wetting-layer system are used in conjunction with a many-body description of Coulomb interaction and carrier phonon interaction. We analyze the carrier-density and temperature dependence of strong excitation-induced energy shifts of the dipole-allowed quantum-dot transitions. © *2009 American Institute of Physics*. [DOI: 10.1063/1.3213543]

Semiconductor quantum dots (QDs) with carrier confinement in all spatial dimensions are regarded as promising candidates for the active material in next generation light-emitting devices. A substantial application potential is found in laser systems[1,2] and for quantum information technologies.[3] Record low threshold current densities, temperature insensitivity, and short pulse capability have been demonstrated for QD lasers.[4–6] For many applications it is beneficial to couple the QD emission to microcavity modes. A three-dimensional confinement of the electromagnetic field can be used to modify the QD emission properties. This has been utilized in structured vertical cavity surface emitting lasers,[7–9] photonic crystals,[10,11] or microdisks.[12]

When QDs are used as active material in optical microresonators, a large spectral overlap between QD emission and cavity modes is required. Especially for laser applications, excitation-induced energy shifts of the optical QD transitions can lower the device efficiency. In this letter, we combine the task to quantify excitation-induced shifts of QD emitters with the more general goal to investigate the combined influence of material properties and interaction effects on optical properties. The predictive power of a microscopic theory improves strongly when the interaction matrix elements are determined from the atomistic structure of the QD emitters. We demonstrate the feasibility of this approach for the InN material system, in which the lattice structure together with the quantum confinement leads to modified optical transitions.

For optoelectronic applications, the group-III nitride material system is of current interest, e.g., due to its wide range of possible emission frequencies. Nitride-based heterostructures are mostly grown on the *c*-plane and predominantly show a wurtzite crystal symmetry. In such devices strong intrinsic electrostatic fields due to spontaneous polarization and piezoelectric effects lead to a reduced efficiency of optical interband transitions.[13,14] Detailed theoretical studies on the influence of such material properties on the electronic structure of QD and quantum-well systems are based on *ab initio*, tight-binding (TB), and $\vec{k}\cdot\vec{p}$ calculations.[15–17] However, these investigations mostly focus on the single-particle properties of nanostructures. From GaAs-based systems it is known that the optical properties are also strongly influenced by many-body effects. Especially in the high carrier-density regime, the interaction with carriers in the energetically nearby continuum of wetting-layer (WL) states is significant.[18–20]

For the description of the single-particle properties of our system a TB model is used. Calculations of bound states are performed for a lens-shaped InN QD grown in the (0001)-direction that is located on top of a InN WL and embedded in a GaN matrix. For the QD-WL structure a diameter of 4.5 nm, a height of 1.6 nm, and a WL thickness of 0.6 nm are considered. The QD structure itself is modeled on a wurtzite lattice of atomic sites. At each lattice site a sp^3-basis is used and the TB parameters are chosen according to the species of the occupying atom (In, Ga, and N). The calculations include the intrinsic electrostatic fields due to spontaneous and strain-induced polarizations. As this work focuses on excitation induced effects in this system, we neglect additional electrostatic fields, that could stem e.g., from bias voltages in electrically pumped devices. Details on the TB model and the resulting QD wave functions are presented in Refs. 16 and 21.

To characterize the delocalized WL states, a separate TB calculation is performed for the WL without QDs, yielding the TB analogs to two-dimensional plane-wave states of a continuum model. The influence of QDs on delocalized WL states is then included via the TB analog of the orthogonalized plane waves scheme, applied in Ref. 22. Within this procedure we are able to account for the random distribution of the QD ensemble on the WL plane. In the following, we consider a QD density of 10^{10} cm^{-2}.

The resulting nonparabolic energy dispersion for WL carriers is presented in Fig. 1. A specific feature of InN is the weak spin-orbit coupling.[23] This, together with the wurtzite symmetry of the crystal lattice, leads to a valence-band structure in which the upper two subbands are nearly degenerate, indicating strong subband mixing.[24,25] Consequently, both subbands of the valence band contribute to the optical properties. For example, the distribution of holes, that strongly influences excitation-induced effects, differs substantially from the one-subband case due to the higher density of states at the band edge. The QD confinement energies are indicated

a)Electronic mail: mlorke@itp.uni-bremen.de.
b)URL: www.itp.uni-bremen.de/ag-jahnke.

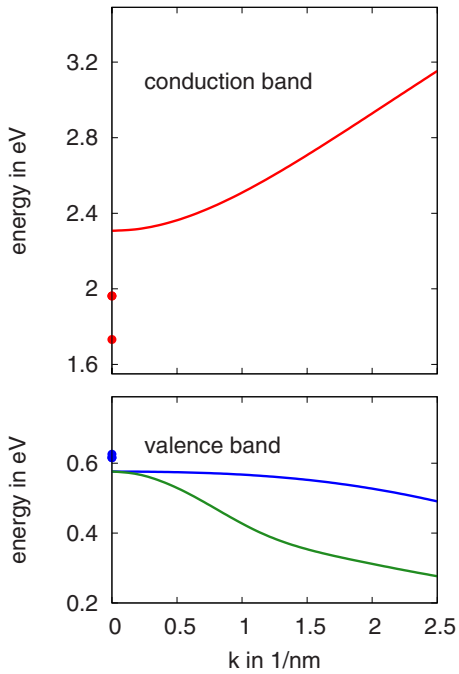

FIG. 1. (Color online) Nonparabolic energy dispersion of the InN WL for the conduction band (a) and the valence band (b) as well as QD energies for electrons and holes (red and blue dots, respectively) obtained from the atomistic TB calculation.

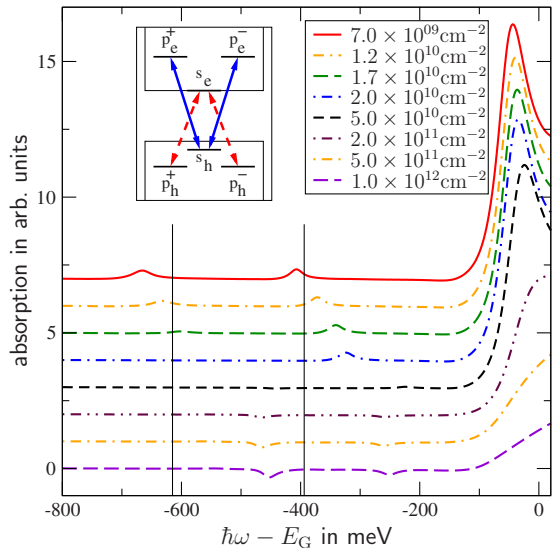

FIG. 2. (Color online) Optical absorption spectra for the InN QD-WL system for a temperature of 300 K and various carrier densities. The spectra are vertically displaced for better visibility. The vertical lines indicate the positions of the skew free-carrier transitions, illustrated in the inset.

as dots in Fig. 1. The InN QD under consideration exhibits deeply confined shells, especially for electrons. The confinement energy for the lowest QD states are −575.4 and −345.3 meV for electrons, and −49.6 and −39.8 meV for holes, relative to the respective WL bandedges.

The coherent optical response of the QD-WL system can be calculated from kinetic equations for the interband transition amplitudes $\psi_{\alpha\beta}=\langle v_\beta^\dagger c_\alpha\rangle$ with the valence electron creation and conduction electron annihilation operators of the states α and β, respectively. The macroscopic optical polarization follows from

$$P = \sum_{\alpha\beta} d_{\alpha\beta}^* \psi_{\alpha\beta} \tag{1}$$

with the dipole coupling $d_{\alpha\beta}$ and determines the linear optical susceptibility $\chi(\omega)=[P(\omega)]/[E(\omega)]$. The kinetic equation for the interband transition amplitudes has the form

$$i\hbar \frac{d}{dt}\psi_{\alpha\beta} = (\tilde{\epsilon}_\alpha^e + \tilde{\epsilon}_\beta^h)\psi_{\alpha\beta} + (1 - f_\alpha^e - f_\beta^h)\tilde{\Omega}_{\alpha\beta}(t) + S_{\alpha\beta}(t). \tag{2}$$

Coulomb effects can be classified into Hartree, exchange and correlation contributions. Different electron and hole populations of the QD states lead to charging effects. The corresponding electrostatic interaction results in Hartree contributions to energy shifts. These Hartree shifts strongly dominate in comparison to the exchange and correlation contributions to the energy shifts. Therefore the latter are included in screened exchange–Coulomb hole (SX-CH) approximation, leading to renormalized single-particle energies $\tilde{\epsilon}_\alpha$. On the same level, renormalized Rabi energies $\tilde{\Omega}_{\alpha\beta}$ are determined.[26] As an approximation to the excitation-induced dephasing we include effects due to carrier interaction with LO-phonons in the polaron picture as described in Ref. 19 via scattering integrals $S_{\alpha\beta}(t)$.

The matrix elements for the Coulomb interaction and the polar coupling of carriers to LO-phonons as well as the selection rules for dipole transitions are evaluated using the wave functions obtained from the atomistic TB calculation, see Refs. 16 and 27. In case of QD-QD interband transitions, we find modified selection rules for the particular QD geometry under consideration. Direct transitions s→s and p→p contribute only weakly in comparison to the off-diagonal transitions s→p and p→s, see inset of Fig. 2. These "skew" transition rules have been confirmed by a group theoretical analysis and their role in multiexciton spectra of InN QDs has been demonstrated in Ref. 27.

Absorption spectra obtained from Eqs. (1) and (2) are shown in Fig. 2 for a successively increasing quasiequilibrium population of electrons and holes. The confinement energies of the QD states in conjunction with the "skew" dipole selection rules correspond to free-carrier transition energies of −615.2 and −394.9 meV relative to the WL bandgap E_G. With increasing carrier density, the energies of the QD absorption lines exhibit a strong blue shift accompanied by bleaching and a transition to optical gain. As can be seen in Fig. 3, the changes of the QD interband transition energies follow mainly the Hartree shifts, which are slightly reduced by the SX terms, while the CH terms do not influence interband transition energies. The Hartree shifts grow with increasing population of the QD states. The population of WL states with electrons and holes leads as a net result to a screening of the QD Hartree interaction.[28] This reduces the Hartree shifts for larger carrier densities so that the net Hartree shift starts do decrease for carrier densities exceeding 5×10^{10} cm^{-2}. The very different confinement potentials for electrons and holes in the considered example result in a population situation, where significantly more electrons than holes are found in the QD states.

In Fig. 4 the peak positions are displayed for two different carrier densities as a function of the temperature. Note that the plots do not include the temperature dependence of

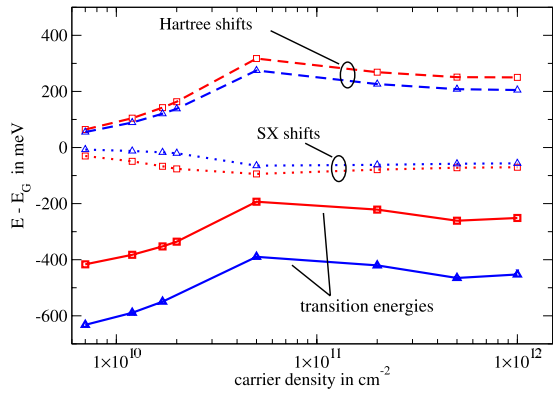

FIG. 3. (Color online) Spectral positions of the QD transitions of Fig. 2 (solid lines) as well as modifications of the single-particle transition energies due to Hartree (dashed line) and screened exchange (dotted line) interaction as a function of the carrier density.

the bandgap E_G to emphasize the energy shifts due to excited carriers. We can infer a drastic increase of the Hartree contributions for decreasing temperature. This behavior can be directly traced back to the QD population. The deep QD confinement potential for the electrons ensures a large quasiequilibrium occupation probability of the QD states already at elevated temperatures and low carrier densities, which does not change for decreasing temperature. In contrast, the shallow hole confinement leads to a strong temperature dependence of the QD population for the hole states. The electrostatic interaction of the increasing hole population with decreasing temperature is responsible for the larger line shifts.

In summary, we investigated the excitation induced shifts of QD transitions in the InN material system. The atomistic TB description of the QD geometry was not only used to determine confinement levels and dipole transitions. Moreover, Coulomb and carrier-phonon interaction matrix elements have been determined from the wave functions of the combined QD and WL system, and used within many-body calculations of the optical properties. The charging of QDs leads to pronounced shifts of the QD resonances in optical absorption spectra due to the interplay of Hartree and exchange interaction. Depending on the carrier density, energy shifts exceeding 200 meV are observed.

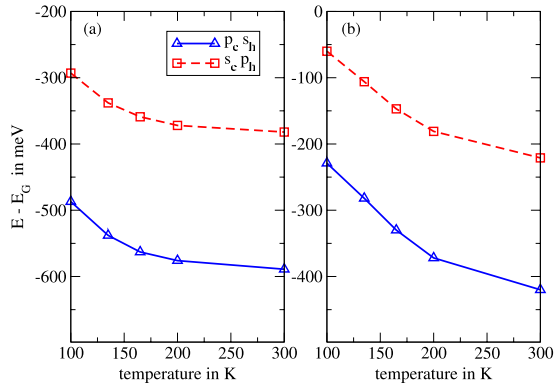

FIG. 4. (Color online) Spectral positions of the QD transitions relative to the WL band edge as a function of temperature for carrier densities of (a) 1.2×10^{10} cm^{-2} and (b) 2.0×10^{11} cm^{-2}.

This work was supported by the Deutsche Forschungsgemeinschaft under Grant No. FOR506 and for CPU time at the NIC, Forschungszentrum Jülich. S.S. acknowledges support from the Humboldt Stiftung and the IRCSET Embark Initiative.

[1] *Self-Assembled InGaAs/GaAs Quantum Dots*, edited by M. Sugawara (Academic, San Diego, 1999).
[2] *Quantum Dot Heterostructures*, edited by D. Bimberg, M. Grundmann, and N. N. Ledenstov (Wiley, New York, 1999).
[3] X. Q. Li, Y. W. Wu, D. Steel, D. Gammonand, T. H. Stievaterand, D. S. Katzer, D. Park, C. Piermarocchi, and L. J. Sham, Science **301**, 809 (2003).
[4] J. Tatebayashi, N. Hatori, H. Kakuma, H. Ebe, H. S. A. K. Y. Nakata, M. Sugawaraand, and Y. Arakawa, Electron. Lett. **39**, 1130 (2003).
[5] S. Deubert, R. Debusmann, J. P. Reithmaier, and A. Forchel, Electron. Lett. **41**, 1125 (2005).
[6] P. M. Smowton, E. J. Pearce, H. C. Schneider, W. W. Chow, and M. Hopkinson, Appl. Phys. Lett. **81**, 3251 (2002).
[7] M. Bayer, F. Weidner, A. Larionov, A. McDonald, A. Forchel, and T. L. Reinecke, Phys. Rev. Lett. **86**, 3168 (2001).
[8] H. Lohmeyer, K. Sebald, C. Kruse, R. Kröger, J. Gutowski, D. Hommel, J. Wiersig, N. Baer, and F. Jahnke, Appl. Phys. Lett. **88**, 051101 (2006).
[9] S. Reitzenstein, A. Bazhenov, A. Gorbunov, C. Hofmann, S. Münch, A. Löffler, M. Kamp, J. P. Reithmaier, V. D. Kulakovskii, and A. Forchel, Appl. Phys. Lett. **89**, 051107 (2006).
[10] P. Lodahl, A. Floris van Driel, I. S. Nikolaev, A. Irman, K. Overgaag, D. Vanmaekelbergh, and W. L. Vos, Nature (London) **430**, 654 (2004).
[11] J.-S. Choi, M. T. Rakher, K. Hennessy, S. Strauf, A. Badolato, P. M. Petroff, E. Hu, and D. Bouwmeester, Appl. Phys. Lett. **91**, 031108 (2007).
[12] Z. G. Xie, S. Götzinger, W. Fang, H. Cao, and G. S. Solomon, Phys. Rev. Lett. **98**, 117401 (2007).
[13] Y.-H. Cho, B. Kwon, J. Barjon, J. Brault, B. Daudin, H. Mariette, and L. Dang, Appl. Phys. Lett. **81**, 4934 (2002).
[14] V. Fonoberov and A. Balandin, J. Appl. Phys. **94**, 7178 (2003).
[15] A. Andreev and E. O'Reilly, Phys. Rev. B **62**, 15851 (2000).
[16] S. Schulz, S. Schumacher, and G. Czycholl, Phys. Rev. B **73**, 245327 (2006).
[17] M. Winkelnkemper, R. Seguin, S. Rodt, A. Schliwa, L. R. mann, A. Strittmatter, A. Hoffmann, and D. Bimberg, J. Appl. Phys. **101**, 113708 (2007).
[18] H. Schneider, W. Chow, and S. Koch, Phys. Rev. B **70**, 235308 (2004).
[19] M. Lorke, T. Nielsen, J. Seebeck, P. Gartner, and F. Jahnke, Phys. Rev. B **73**, 085324 (2006).
[20] M. Lorke, W. W. Chow, T. R. Nielsen, J. Seebeck, P. Gartner, and F. Jahnke, Phys. Rev. B **74**, 035334 (2006).
[21] S. Schulz, S. Schumacher, and G. Czycholl, Eur. Phys. J. B **64**, 51 (2008).
[22] T. Nielsen, P. Gartner, and F. Jahnke, Phys. Rev. B **69**, 235314 (2004).
[23] I. Vurgaftman and J. Meyer, J. Appl. Phys. **94**, 3675 (2003).
[24] S. Schulz, S. Schumacher, and G. Czycholl, Phys. Status Solidi B **244**, 2399 (2007).
[25] S. Chuang and C. Chang, Phys. Rev. B **54**, 2491 (1996).
[26] H. Haug and S. W. Koch, *Quantum Theory of the Optical and Electronic Properties of Semiconductors*, 4th ed. (World Scientific, Singapore, 2004).
[27] N. Baer, S. Schulz, S. Schumacher, P. Gartner, G. Czycholl, and F. Jahnke, Appl. Phys. Lett. **87**, 231114 (2005).
[28] T. Nielsen, P. Gartner, M. Lorke, J. Seebeck, and F. Jahnke, Phys. Rev. B **72**, 235311 (2005).